

# Enhancing Geometric Ontology Embeddings for $\mathcal{EL}^{++}$ with Negative Sampling and Deductive Closure Filtering

Olga Mashkova<sup>1</sup>[0000–0002–4916–1660], Fernando  
Zhapa-Camacho<sup>1</sup>[0000–0002–0710–2259], and Robert  
Hoehndorf<sup>1</sup>[0000–0001–8149–5890]

Computer Science Program, Computer, Electrical, and Mathematical Sciences &  
Engineering Division, King Abdullah University of Science and Technology, Thuwal  
23955, Saudi Arabia

{olga.mashkova,fernando.zhapacamacho,robert.hoehndorf}@kaust.edu.sa

**Abstract.** Ontology embeddings map classes, relations, and individuals in ontologies into  $\mathbb{R}^n$ , and within  $\mathbb{R}^n$  similarity between entities can be computed or new axioms inferred. For ontologies in the Description Logic  $\mathcal{EL}^{++}$ , several embedding methods have been developed that explicitly generate models of an ontology. However, these methods suffer from some limitations; they do not distinguish between statements that are unprovable and provably false, and therefore they may use entailed statements as negatives. Furthermore, they do not utilize the deductive closure of an ontology to identify statements that are inferred but not asserted. We evaluated a set of embedding methods for  $\mathcal{EL}^{++}$  ontologies based on high-dimensional ball representation of concept descriptions, incorporating several modifications that aim to make use of the ontology deductive closure. In particular, we designed novel negative losses that account both for the deductive closure and different types of negatives. We demonstrate that our embedding methods improve over the baseline ontology embedding in the task of knowledge base or ontology completion.

**Keywords:** Ontology Embedding · Knowledge Base Completion · Description Logic  $\mathcal{EL}^{++}$ .

## 1 Introduction

Several methods have been developed to embed Description Logic theories or ontologies in vector spaces [5, 6, 13, 18, 23, 24, 25, 30]. These embedding methods preserve some aspects of the semantics in the vector space, and may enable the computation of semantic similarity, inferring axioms that are entailed, and predicting axioms that are not entailed but may be added to the theory. For the lightweight Description Logic  $\mathcal{EL}^{++}$ , several geometric embedding methods have been developed [13, 18, 23, 24, 30]. They can be proven to “faithfully” approximate a model in the sense that, if a certain optimization objective is reached

(usually, a loss function reduced to 0), the embedding method has constructed a model of the  $\mathcal{EL}^{++}$  theory. Geometric model construction enables the execution of various tasks. These tasks include knowledge base completion and subsumption prediction via either testing the truth of a statement under consideration in a single (approximate) model or aggregating truth values over multiple models.

Advances on different geometric embedding methods have usually focused on the expressiveness of the embedding methods; originally, hyperballs[18] were used to represent the interpretation of concept symbols, yet hyperballs are not closed under intersection. Therefore, axis-aligned boxes were introduced [13, 25, 30]. Furthermore,  $\mathcal{EL}^{++}$  allows for axioms pertaining to relations, and several methods have extended the way in which relations are modeled [13, 18, 30]. However, there are several aspects of geometric embeddings that have not yet been investigated. In particular, for  $\mathcal{EL}^{++}$ , there are sound and complete reasoners with efficient implementations that scale to very large knowledge bases [16]; it may therefore be possible to utilize a deductive reasoner together with the embedding process to improve generation of embeddings that represent geometric models.

We evaluate geometric embedding methods and incorporate deductive inference into the training process. We use the *ELEmbeddings* [18] model for our experiments due to its simplicity; however, our results also apply to other geometric embedding methods for  $\mathcal{EL}^{++}$ .

Our main contributions are as follows:

- We investigate and reveal biases in some evaluation datasets that are related to how the task of knowledge base completion is formulated, and demonstrate that, due to these biases, even when models collapse, predictive performance can be high.
- We introduce loss functions that avoid zero gradients and improve the task of knowledge base completion.
- We introduce a fast approximate algorithm for computing the deductive closure of an  $\mathcal{EL}^{++}$  theory and use it to improve negative sampling during model training.
- We propose loss functions that incorporate negative samples in most normal forms.

## 2 Preliminaries

### 2.1 Description Logic $\mathcal{EL}^{++}$

Let  $\Sigma = (\mathbf{C}, \mathbf{R}, \mathbf{I})$  be a signature with set  $\mathbf{C}$  of concept names,  $\mathbf{R}$  of role names, and  $\mathbf{I}$  of individual names. Given  $A, B \in \mathbf{C}$ ,  $r \in \mathbf{R}$ , and  $a, b \in \mathbf{I}$ ,  $\mathcal{EL}^{++}$  concept descriptions are constructed with the grammar  $\perp \mid \top \mid A \sqcap B \mid \exists r.A \mid \{a\}$ . ABox axioms are of the form  $A(a)$  and  $r(a, b)$ , TBox axioms are of the form  $A \sqsubseteq B$ , and RBox axioms are of the form  $r_1 \circ r_2 \circ \dots \circ r_n \sqsubseteq r$ .  $\mathcal{EL}^{++}$  *generalized concept inclusions* (GCIs) and *role inclusions* (RIs) can be normalized to follow one of these forms [1]:  $C \sqsubseteq D$  (GCI0),  $C \sqcap D \sqsubseteq E$  (GCI1),  $C \sqsubseteq \exists R.D$  (GCI2),

$\exists R.C \sqsubseteq D$  (GCI3),  $C \sqsubseteq \perp$  (GCI0-BOT),  $C \sqcap D \sqsubseteq \perp$  (GCI1-BOT),  $\exists R.C \sqsubseteq \perp$  (GCI3-BOT) and  $r \sqsubseteq s$  (RI0),  $r_1 \circ r_2 \sqsubseteq s$  (RI1), respectively.

To define the semantics of an  $\mathcal{EL}^{++}$  theory, we use [1] an *interpretation domain*  $\Delta^{\mathcal{I}}$  and an *interpretation function*  $\cdot^{\mathcal{I}}$ . For every concept  $A \in \mathbf{C}$ ,  $A^{\mathcal{I}} \subseteq \Delta^{\mathcal{I}}$ ; individual  $a \in \mathbf{I}$ ,  $a^{\mathcal{I}} \in \Delta^{\mathcal{I}}$ ; role  $r \in \mathbf{R}$ ,  $r^{\mathcal{I}} \in \Delta^{\mathcal{I}} \times \Delta^{\mathcal{I}}$ . Furthermore, the semantics for other  $\mathcal{EL}^{++}$  constructs are the following (omitting concrete domains and role inclusions):

$$\begin{aligned}
 \perp^{\mathcal{I}} &= \emptyset \\
 \top^{\mathcal{I}} &= \Delta^{\mathcal{I}}, \\
 (A \sqcap B)^{\mathcal{I}} &= A^{\mathcal{I}} \cap B^{\mathcal{I}}, \\
 (\exists r.A)^{\mathcal{I}} &= \{a \in \Delta^{\mathcal{I}} \mid \exists b : ((a, b) \in r^{\mathcal{I}} \wedge b \in A^{\mathcal{I}})\}, \\
 (a)^{\mathcal{I}} &= \{a\}
 \end{aligned}$$

An interpretation  $\mathcal{I}$  is a model for an axiom  $C \sqsubseteq D$  if and only if  $C^{\mathcal{I}} \subseteq D^{\mathcal{I}}$ , for an axiom  $B(a)$  if and only if  $a^{\mathcal{I}} \in B^{\mathcal{I}}$ ; and for an axiom  $r(a, b)$  if and only if  $(a^{\mathcal{I}}, b^{\mathcal{I}}) \in r^{\mathcal{I}}$  [2].

## 2.2 Knowledge Base Completion

The task of knowledge base completion is the addition (or prediction) of axioms to a knowledge base that are not explicitly represented. We call the task “ontology completion” when exclusively TBox axioms are predicted. The task of knowledge base completion may encompass both deductive [15, 27] and inductive [3, 10] inference processes and give rise to two subtly different tasks: adding only “novel” axioms to a knowledge base that are *not* in the deductive closure of the knowledge base, and adding axioms that are in the deductive closure as well as some “novel” axioms that are not deductively inferred; both tasks are related but differ in how they are evaluated.

Inductive inference, analogously to knowledge graph completion [7], predicts axioms based on patterns and regularities within the knowledge base. Knowledge base completion, or ontology completion, can be further distinguished based on the information that is used to predict “novel” axioms. We distinguish between two approaches to knowledge base completion: (1) knowledge base completion which relies solely on (formalized) information within the knowledge base to predict new axioms, and (2) knowledge base completion which incorporates side information, such as text, to enhance the prediction of new axioms. Here, we mainly consider the first case.

## 3 Related Work

### 3.1 Graph-Based Ontology Embeddings

Graph-based ontology embeddings rely on a construction (projection) of graphs from ontology axioms mapping ontology classes, individuals and roles to nodes

and labeled edges [31]. Embeddings for nodes and edge labels are optimized using Knowledge Graph Embedding (KGE) methods [29]. These type of methods have been shown effective on knowledge base and ontology completion [5] and have been applied to domain-specific tasks such as protein–protein interaction prediction [5] or gene–disease association prediction [6]. Graph-based methods rely on adjacency information of the ontology structure but cannot easily handle logical operators and do not approximate ontology models. Therefore, graph-based methods are not “faithful”, i.e., do not approximate models, do not allow determining whether statements are “true” in these models, and therefore cannot be used to perform semantic entailment.

### 3.2 Geometric-Based Ontology Embeddings

Multiple methods have been developed for the geometric construction of models for the  $\mathcal{EL}^{++}$  language. ELEmbeddings [18] constructs an interpretation of concept names as sets of points lying within an open  $n$ -dimensional ball and generates an interpretation of role names as the set of pairs of points that are separated by a vector in  $\mathbb{R}^n$ , i.e., by the embedding of the role name. EmEL++ [23] extends ELEmbeddings with more expressive constructs such as role chains and role inclusions. ELBE [25] and BoxEL [30] use  $n$ -dimensional axis-aligned boxes to represent concepts, which has an advantage over balls because the intersection of two axis-aligned boxes is a box whereas the intersection of two  $n$ -balls is not an  $n$ -ball. BoxEL additionally preserves ABox facilitating a more accurate representation of knowledge base’s logical structure by ensuring, e.g., that an entity has the minimal volume. Box<sup>2</sup>EL [13] represents ontology roles more expressively with two boxes encoding the semantics of the domain and codomain of roles. Box<sup>2</sup>EL enables the expression of one-to-many relations as opposed to other methods. Axis-aligned cone-shaped geometric model introduced in [24] deals with  $\mathcal{ALC}$  ontologies and allows for full negation of concepts and existential quantification by construction of convex sets in  $\mathbb{R}^n$ . This work has not yet been implemented or evaluated in an application.

### 3.3 Knowledge Base Completion Task

Several recent advancements in the knowledge base completion rely on side information as included in Large Language Models (LLMs). [14] explores how pretrained language models can be utilized for incorporating one ontology into another, with the main focus on inconsistency handling and ontology coherence. HalTon [4] addresses the task of event ontology completion via simultaneous event clustering, hierarchy expansion and type naming utilizing BERT [9] for instance encoding. [19] formulates knowledge base completion task as a Natural Language Inference (NLI) problem and examines how this approach may be combined with concept embeddings for identifying missing knowledge in ontologies. As for other approaches, [22] proposes a method that converts an ontology into a graph to recommend missing edges using structure-only link analysis methods, [28] constructs matrix-based ontology embeddings which capture the global and

local information for subsumption prediction. All these methods use side information from LLMs and would not be applicable, for example, in the case where a knowledge base is private or consists of only identifiers; we do not consider methods based on pre-trained LLMs here as baselines.

## 4 Methods

### 4.1 Datasets

Following previous works [13, 18, 25] we use common benchmarks for the prediction of protein-protein interactions (PPIs). We also reorganize the same data for the task of protein function prediction. For our experiments we use four datasets; each of them consists of the Gene Ontology [8] with all its axioms, protein-protein interactions (PPIs) and protein function axioms extracted from the STRING database [21]; we use one dataset focusing on only yeast and another dataset focusing on only human proteins. GO is formalized using OWL 2 EL [11].

For PPI yeast network we use the built-in dataset `PPIYeastDataset` available in the `mOWL` [32] Python library (release 0.2.1) where axioms of interest are split randomly into train, validation and test datasets in ratio 90:5:5 keeping pairs of symmetric PPI axioms within the same dataset, and other axioms are placed into the training part; validation and test sets are made up of TBox axioms of type  $\{P_1\} \sqsubseteq \exists \textit{interacts\_with}.\{P_2\}$  where  $P_1, P_2$  are protein names. In case of yeast proteins, the GO version released on 2021-10-20 and the STRING database version 11.5 were used. Alongside with the yeast *interacts\_with* dataset we collected the yeast *has\_function* dataset organized in the same manner with validation and test parts containing TBox axioms of type  $\{P\} \sqsubseteq \exists \textit{has\_function}.\{GO\}$ . The human *interacts\_with* and *has\_function* datasets were built from STRING PPI human network (version 10.5) and GO released on 2018-12-28. Based on the information in the STRING database, in PPI yeast, the *interacts\_with* relation is symmetric and the dataset is closed against symmetric interactions; the PPI human dataset does not always contain the inverse of interactions and is not closed against symmetry. We normalize all ontology axioms using the implementation of the `jcel` [20] reasoner, accessed through the `mOWL` library [32]. Role inclusion axioms are ignored since we experiment with modifications of the *ELEmbeddings* method where role inclusion axioms are omitted as well. The number of GCIs of each type in the datasets can be found in the Appendix B.

### 4.2 Objective Functions

*ELEmbeddings* use a single loss for “negatives”, i.e., axioms that are not included in the knowledge base; the loss is used only for axioms of the form  $C \sqsubseteq \exists R.D$  which are randomly sampled, and negatives are not considered for other normal forms. We add three more “negative” losses:  $C \sqsubseteq D$ ,  $C \sqcap D \sqsubseteq E$ , and  $\exists R.C \sqsubseteq D$ :

$$\begin{aligned}
& loss_{C \sqsubseteq D}(c, d) = \\
& = l(r_\eta(c) + r_\eta(d) - \|f_\eta(c) - f_\eta(d)\| + \gamma) + \\
& \quad + |\|f_\eta(c)\| - 1| + |\|f_\eta(d)\| - 1|
\end{aligned} \tag{1}$$

$$\begin{aligned}
& loss_{C \cap D \sqsubseteq E}(c, d, e) = \\
& = l(-r_\eta(c) - r_\eta(d) + \|f_\eta(c) - f_\eta(d)\| - \gamma) + \\
& \quad + l(r_\eta(c) - \|f_\eta(c) - f_\eta(e)\| + \gamma) + \\
& \quad + l(r_\eta(d) - \|f_\eta(d) - f_\eta(e)\| + \gamma) + \\
& \quad + |\|f_\eta(c)\| - 1| + |\|f_\eta(d)\| - 1| + |\|f_\eta(e)\| - 1|
\end{aligned} \tag{2}$$

$$\begin{aligned}
& loss_{\exists R.C \sqsubseteq D}(r, c, d) = \\
& = l(r_\eta(c) + r_\eta(d) - \|f_\eta(c) - f_\eta(r) - f_\eta(d)\| + \gamma) + \\
& \quad + |\|f_\eta(c)\| - 1| + |\|f_\eta(d)\| - 1|
\end{aligned} \tag{3}$$

Here,  $l$  denotes a function that determines the behavior of the loss when the axiom is true (for positive cases) or not true (for negative cases); in our case, we consider ReLU and LeakyReLU;  $\gamma$  stands for a margin parameter. We employ notations from the *ELEmbeddings* method:  $r_\eta(c)$ ,  $r_\eta(d)$ ,  $r_\eta(e)$  and  $f_\eta(c)$ ,  $f_\eta(d)$ ,  $f_\eta(e)$  denote the radius and the ball center associated with classes  $c$ ,  $d$ ,  $e$ , respectively,  $f_\eta(r)$  denotes the embedding vector associated with relation  $r$ . There is a geometrical part as well as a regularization part for each new negative loss forcing class centers to lie on a unit  $\ell_2$ -sphere. Negative loss 3 is constructed similarly to  $C \cap D \sqsubseteq E$  loss: the first part penalizes non-overlap of  $C$  and  $D$  classes (we do not consider disjointness case since for every class  $X$  we have  $\perp \sqsubseteq X$ ); the second and the third part force the center corresponding to  $E$  not to lie in the intersection of balls associated with  $C$  and  $D$ . Here we do not consider constraints on radius of the ball for  $E$  class and focus only on relative positions of  $C$ ,  $D$  and  $E$  class centers and overlapping of  $n$ -balls representing  $C$  and  $D$ . In our experiments, we also use a relaxed regularization where  $\|f_\eta(c)\| = R$  is replaced with  $\|f_\eta(c)\| \leq R$  on  $n$ -ball centers representing concepts forcing them to lie inside the corresponding closed ball of radius  $R$  centered at 0. Relaxed version of regularization may allow for more accurate representation of a knowledge base since it is not forcing all ball centers corresponding to concept names to lie on a unit sphere.

### 4.3 Deductive Closure: Negatives Filtration

The *deductive closure* of a theory  $T$  refers to the smallest set containing all statements which can be inferred by deductive reasoning over  $T$ ; for a given deductive relation  $\vdash$ , we call  $T^\vdash = \{\phi \mid T \vdash \phi\}$  the deductive closure of  $T$ . In knowledge bases, the deductive closure is usually not identical to the asserted

axioms in the knowledge base, and will contain axioms that are non-trivial; it is also usually infinite.

Representing the deductive closure is challenging since it is infinite, but in  $\mathcal{EL}^{++}$  any knowledge base can be normalized to one of the seven normal forms; therefore, we can compute the deductive closure with respect to these normal forms. However, existing  $\mathcal{EL}^{++}$  reasoners such as ELK [16] compute all axioms of the form  $C \sqsubseteq D$  in the deductive closure but not the other normal forms. We use the inferences computed by ELK (of the form  $C \sqsubseteq D$ ) to design an algorithm that computes the deductive closure with respect to the  $\mathcal{EL}^{++}$  normal forms; the algorithm implements sound but incomplete inference rules (see Algorithm 1 for further details); specifically, it computes entailed axioms for all normal forms based on the concept hierarchy pre-computed by ELK.

#### 4.4 Training Procedure

To address the issue of data imbalance (see Appendix B), i.e., the imbalance between the number of axioms of different normal forms represented in a knowledge base which may have an impact on how well certain types of axioms are represented in the embedding space, we weigh individual GCI losses based on frequency of the axiom types sampled during one epoch. All models are optimized with respect to the weighted sum of individual GCI losses (here we define the loss in most general case using all positive and all negative losses):

$$\begin{aligned} \mathcal{L} = & w_{C \sqsubseteq D} \cdot l_{C \sqsubseteq D} + w_{C \cap D \sqsubseteq E} \cdot l_{C \cap D \sqsubseteq E} + w_{C \sqsubseteq \exists R.D} \cdot l_{C \sqsubseteq \exists R.D} + \\ & + w_{\exists R.C \sqsubseteq D} \cdot l_{\exists R.C \sqsubseteq D} + w_{C \sqsubseteq \perp} \cdot l_{C \sqsubseteq \perp} + w_{\exists R.C \sqsubseteq \perp} \cdot l_{\exists R.C \sqsubseteq \perp} + \\ & + w_{C \not\sqsubseteq D} \cdot l_{C \not\sqsubseteq D} + w_{C \cap D \not\sqsubseteq E} \cdot l_{C \cap D \not\sqsubseteq E} + w_{C \not\sqsubseteq \exists R.D} \cdot l_{C \not\sqsubseteq \exists R.D} + \\ & + w_{\exists R.C \not\sqsubseteq D} \cdot l_{\exists R.C \not\sqsubseteq D} \end{aligned} \quad (4)$$

To study the phenomenon of biases in data affecting model training and performance, we build a ‘naive’ model which predicts only based on the frequency with which a class appears in an axiom. Intuitively, it is designed to resemble predictions based on node degree in knowledge graphs:

$$score_{C \sqsubseteq \exists R.D}(c, r, d) = \frac{\sum_{c'} M_r(c', d)}{\sum_{k, l} M_r(k, l)} \quad (5)$$

All model architectures are built using mOWL [32] library on top of mOWL’s base models. All models were trained using the same fixed random seed. Training code for all experiments and models is available on <https://github.com/bio-ontology-research-group/geometric-embeddings>.

All models are trained for 400 epochs with batch size of 32,768. Training and optimization is performed using Pytorch with Adam optimizer [17] and ReduceLROnPlateau scheduler with patience parameter 10. We apply early stopping if validation loss does not improve for 20 epochs. Hyperparameters are tuned using grid search over the following set: margin  $\gamma \in \{-0.1, -0.01, 0, 0.01, 0.1\}$ , embedding dimension  $\{50, 100, 200, 400\}$ , regularization radius  $R \in \{1, 2\}$ , learning

rate  $\{0.01, 0.001, 0.0001\}$ . For *ELEmbeddings*, the strict version of regularization  $\|f_\eta(c)\| = R$  was used with  $R = 1$ ; see Appendix C for details on optimal hyperparameters used.

#### 4.5 Evaluation score and metrics

We predict GCI2 axioms of type  $\{P_1\} \sqsubseteq \exists \textit{interacts\_with}.\{P_2\}$  or  $\{P\} \sqsubseteq \sqsubseteq \exists \textit{has\_function}.\{GO\}$  depending on the dataset. As the core evaluation score we use the scoring function introduced in *ELEmbeddings*:

$$\begin{aligned} \textit{score}_{C \sqsubseteq \exists R.D}(c, r, d) &= \\ &= -l(-r_\eta(c) - r_\eta(d) + \|f_\eta(c) + f_\eta(r) - f_\eta(d)\| - \gamma) \end{aligned} \quad (6)$$

The predictive performance is measured by Hits@n metrics for  $n = 10, 100$ , macro and micro mean rank and area under ROC curve (AUC ROC). For rank-based metrics, we calculate the score of  $C \sqsubseteq \exists R.D$  for every class  $C$  from the test set and for every  $D$  from the set  $\mathbf{C}$  of all classes (or subclasses of a certain type, such as proteins or functions) and determine the rank of a test axiom  $C \sqsubseteq \exists R.D$ . For macro mean rank and AUC ROC we consider all axioms from the test set whereas for micro metrics we compute corresponding class-specific metrics averaging them over all classes in the signature:

$$\textit{micro\_MR} = \textit{Mean}(\textit{MR}_C(\{C \sqsubseteq \exists R.D, D \in \mathbf{C}\})) \quad (7)$$

$$\textit{micro\_AUC\_ROC} = \textit{Mean}(\textit{AUC\_ROC}_C(\{C \sqsubseteq \exists R.D, D \in \mathbf{C}\})) \quad (8)$$

Additionally, we remove axioms represented in the train set and obtain corresponding filtered metrics (FHits@n, FMR, FAUC).

## 5 Results

Geometric methods such as *ELEmbeddings* address the task of knowledge base completion by constructing a single (approximate) model for a knowledge base and determining the truth of statements in this model based on geometric scoring functions. However, a single model does not suffice to compute entailments, or approximate entailments. In first order logic or more expressive Description Logics, it is possible to reduce entailment to the task of finding a single model, but since  $\mathcal{EL}^{++}$  does not allow for explicit negation, this approach does not work; furthermore, reducing entailment to consistency (i.e., not having a model) relies on solving an optimization problem (“finding a model”) to compute each entailment. Therefore, geometric methods only construct a single model; the assumption is that any entailed statement has to be true in this model, and some non-entailed statements will also be true. The success of this approach relies on the model being sufficiently expressive, and not constructing “trivial” models of knowledge bases.

Table 1: *ELEmbeddings* experiments: the first column corresponds to the original model, the second one – to LeakyReLU replacement and soft regularization, the third – to GCI0-GCI3 losses added, and, finally, the last one – to negatives filtering. *iw* refers to *interacts\_with* dataset, *hf* – to *has\_function* dataset.

		ReLU	Leaky+Reg	Losses	Neg. filter
Yeast iw	FHits@10	0.00	0.26	0.25	<b>0.29</b>
	FHits@100	0.15	0.74	0.74	<b>0.78</b>
	macro_FMR	287.06	182.93	185.81	<b>172.80</b>
	macro_FAUC	0.95	<b>0.97</b>	<b>0.97</b>	<b>0.97</b>
Yeast hf	FHits@10	0.00	<b>0.25</b>	0.23	0.24
	FHits@100	0.00	<b>0.55</b>	0.54	0.54
	macro_FMR	5183.01	3211.80	<b>2869.43</b>	2875.67
	macro_FAUC	0.90	<b>0.94</b>	<b>0.94</b>	<b>0.94</b>
Human iw	FHits@10	0.00	<b>0.02</b>	0.00	0.00
	FHits@100	0.03	0.24	0.50	<b>0.63</b>
	macro_FMR	490.09	1361.12	258.17	<b>196.76</b>
	macro_FAUC	0.97	0.93	<b>0.99</b>	<b>0.99</b>
Human hf	FHits@10	0.00	<b>0.14</b>	0.06	0.06
	FHits@100	0.00	<b>0.35</b>	0.28	0.28
	macro_FMR	7642.15	4059.81	2270.35	<b>2261.06</b>
	macro_FAUC	0.85	0.92	<b>0.95</b>	<b>0.95</b>

Table 2: Naive approach vs *ELEmbeddings* with LeakyReLU, soft regularization constraints, GCI0-GCI3 negative losses and filtered negatives. *iw* refers to *interacts\_with* dataset, *hf* – to *has\_function* dataset. For Human iw dataset we report here metrics for  $M'_{iw}$ , *sym* here corresponds to the symmetric Human iw dataset (for further details see Appendix (section A)).

		Naive	ELEm
Yeast iw	FHits@10	0.05	<b>0.29</b>
	FHits@100	0.23	<b>0.78</b>
	macro_FMR	1174.33	<b>172.80</b>
	macro_FAUC	0.81	<b>0.97</b>
Yeast hf	FHits@10	0.21	<b>0.24</b>
	FHits@100	0.41	<b>0.54</b>
	macro_FMR	<b>2690.58</b>	2875.67
	macro_FAUC	<b>0.95</b>	0.94
Human iw (sym)	FHits@10	<b>0.02</b>	0.00
	FHits@100	0.08	<b>0.63</b>
	macro_FMR	2299.09	<b>196.76</b>
	macro_FAUC	0.88	<b>0.99</b>
Human hf	FHits@10	<b>0.18</b>	0.06
	FHits@100	<b>0.39</b>	0.28
	macro_FMR	<b>1967.45</b>	2261.06
	macro_FAUC	<b>0.96</b>	0.95

We use the *ELEmbeddings* method to perform knowledge base completion in two applications which are used widely to benchmark geometric ontology embedding methods, predicting protein–protein interactions and predicting protein functions (see Table 1; Appendix Figure 9 shows the resulting ROC curves). To evaluate learned embeddings under different modifications we run the original *ELEmbeddings* model and use the obtained results instead of extracting metrics from the original paper [18]. This is also motivated by the utilization of different versions of GO and STRING database in our work compared to the original paper [18]. We additionally perform an ablation study to evaluate the effect of individual modifications (see Appendix G). We observe that *ELEmbeddings* ranks thousands of axioms at the same rank (i.e., scores them as “true”), and mainly achieves its performance (measured in AUC) by ranking rare protein functions, or proteins that interact rarely, at lower ranks. To further substantiate this hypothesis, we developed a “naive” classifier that predicts solely based on the number of times a class appears as part of an axiom during training; Table 2 shows the results and demonstrates that only based on frequency of a class, a predictive performance close to the actual performance of *ELEmbeddings* can be achieved.

We first investigate whether a relaxation of the loss functions to ensure non-zero gradients at all times can improve performance in the knowledge base completion task. The loss functions are designed to construct a model, and once an axiom from the knowledge base is true in the constructed model, their losses remain zero; however, it may be useful to provide a small gradient even once axioms are true in the constructed model. For this purpose, we change the ReLU function used in constructing losses to a LeakyReLU function. First, we study the effect of replacing ReLU function with LeakyReLU together with relaxed version of regularization (see Table 1; Appendix E for full results). Since LeakyReLU prevents gradients from being stuck at zero, we expect the improvement of model’s performance. Likewise, not forcing the centers of  $n$ -balls representing concepts increases the expressiveness of the model. We demonstrate that, in general, incorporating LeakyReLU and relaxing regularization improves the performance of the initial model allowing learnable concepts to receive gradients at all times and, as a consequence, construct a better approximate model. Furthermore, a LeakyReLU adds the potential for optimization beyond “truth” (i.e., where statements are true in the constructed model and receive no further updates that improve the task of knowledge base completion).

While the LeakyReLU improves the predictive performance of *ELEmbeddings* in the task of knowledge base completion, it does not prevent models from collapsing, i.e., generating trivial models (see Appendix section I). The original *ELEmbeddings* model and other geometric models only use negative losses (i.e., losses for the case that an axiom does not hold) for a single normal form (GCI2,  $C \sqsubseteq \exists R.D$ , which is also used for prediction). We evaluate whether adding negative losses for other normal forms will prevent the model from collapsing and improve the performance in the task of knowledge base completion. We formulate and add GCI0-GCI3 negative losses given by equations 1–3, either separately or

with LeakyReLU and soft regularization from the previous experiment. We find that just adding the additional losses improves the performance and seems to prevent models from collapsing (Appendix Figure 10). In terms of mean rank and AUC ROC, the model with the negative losses generally exhibits improved performance relative to using only negative losses for GCI2.

Similarly to how negative sampling works in knowledge graph completion, geometric ontology embedding methods select negatives by corrupting an axiom by replacing one of the classes with a randomly chosen one; in the case of knowledge base completion where the deductive closure contains potentially many non-trivial entailed axioms, this approach may lead to suboptimal learning since some of axioms treated as negatives are entailed (and will therefore be true in any model, in particular the one constructed by the geometric embedding method). We suggest to filter selected negatives based on the deductive closure of the knowledge base: for each randomly generated axiom to be used as negative, we check whether it is present in the deductive closure and if it is, we delete it. To compute the deductive closure, we use an approximate algorithm (see Appendix J). Table 1 shows results in the tasks we evaluate. We find that excluding axioms in the deductive closure for negative selection improves the results in the task of predicting PPIs, and yields similar results in function prediction tasks. One possible reason is that a randomly chosen axiom is very unlikely to be entailed since very few axioms are entailed compared to all possible axioms to choose from.

Because the chance of selecting an entailed axiom as a negative depends on the knowledge base on which the embedding method is applied, we perform additional experiments where we bias the selection of negatives; we chose between 100% negatives to 0% negatives from the entailed axioms. We find that reducing the number of entailed axioms from the negatives has an effect to improve performance and the effect increases the more axioms would be chosen from the entailed ones (Appendix Figure 11).

The deductive closure can also be used to modify the evaluation metrics. So far, ontology embedding methods that have been applied to the task of knowledge base completion have used evaluation measures that are taken from the task of knowledge graph completion; in particular, they only evaluate knowledge base completion using axioms that are “novel” and not entailed. However, any entailed axiom will be true in all models of the knowledge base, and therefore also in the geometric model that is constructed by the embedding method. These entailed axioms should therefore be considered in the evaluation. We show the difference in performance, and the corresponding ROC curves, in Appendix Figure 12. We find that methods that explicitly construct models generally predict entailed axioms first, even when the models make some trivial predictions (such as in the original *ELEmbeddings* model); model-generating embedding first predict the entailed axioms, and then predict “novel” axioms that are not entailed. However, when replacing the ReLU with the LeakyReLU in *ELEmbeddings*, “novel”, non-entailed axioms are predicted first, before entailed axioms are predicted (see Appendix Figure 13). We evaluate a more recent ontology embedding method

*Box<sup>2</sup>EL* [13] and find that this model predicts primarily “novel” axioms but does not predict entailed axioms (see Appendix Figure 14).

## 6 Discussion

We evaluated properties of *ELEmbeddings*, an ontology embedding method that aims to generate a model of an  $\mathcal{EL}^{++}$  theory; the properties we evaluate hold similarly for other ontology embedding methods that construct models of  $\mathcal{EL}^{++}$  theories. While we demonstrate several improvements over the original model, we can also draw some general conclusions about ontology embedding methods and their evaluation. Knowledge base completion is the task of predicting axioms that should be added to a knowledge base; this task is adapted from knowledge graph completion where triples are added to a knowledge graph. The way both tasks are evaluated is by removing some statements (axioms or triples) from the knowledge base, and evaluating whether these axioms or triples can be recovered by the embedding method. This evaluation approach is adequate for knowledge graphs which do not give rise to many entailments. However, knowledge bases give rise to potentially many non-trivial entailments that need to be considered in the evaluation. In particular embedding methods that aim to generate a model of a knowledge base will first generate entailed axioms (because entailed axioms are true in all models); these methods perform knowledge base completion as a generalization of generating the model where either other statements may be true, or they may be approximately true in the generated structure. This has two consequences: the evaluation procedure needs to account for this; and the model needs to be sufficiently rich to allow useful predictions.

We have introduced a method to compute the deductive closure of  $\mathcal{EL}^{++}$  knowledge bases; this method relies on an automated reasoner and is sound but not complete. We use all the axioms in the deductive closure as positive axioms to be predicted when evaluating knowledge base completion, to account for methods that treat knowledge base completion as a generalization of constructing a model and testing for truth in this model. We find that some models (e.g., the original *ELEmbedding* model) can predict entailed axioms well, some (a modified model using a LeakyReLU function as part of the loss instead of the ReLU) preferentially predict “novel”, non-entailed axioms, and others (e.g., the *Box<sup>2</sup>EL* model) are tailored to predict primarily “novel” knowledge and do not predict entailed axioms; these methods solve subtly different problems (either generalizing construction of a model, or specifically predicting novel non-entailed axioms). We also modify the evaluation procedure to account for the inclusion of entailed axioms as positives; however, the evaluation measures are still based on ranking individual axioms and do not account for semantic similarity. For example, if during testing, the correct axiom to predict is  $C \sqsubseteq \exists R.D$  but the predicted axiom is  $C \sqsubseteq \exists R.E$ , the prediction may be considered to be “more correct” if  $D \sqsubseteq E$  was in the knowledge base than if  $D \sqcap E \sqsubseteq \perp$  was in the knowledge base. Novel evaluation metrics need to be designed to account for this phenomenon, similarly to ontology-based evaluation measures used in life

sciences [26]. It is also important to expand the set of benchmark sets for knowledge base completion.

Use of the deductive closure is not only useful in evaluation but also when selecting negatives. In formal knowledge bases, there are at least two ways in which negatives for axioms can be chosen: they are either non-entailed axioms, or they are axioms whose negation is entailed. However, in no case should entailed axioms be considered as negatives; we demonstrate that filtering entailed axioms from selected negatives during training improves the performance of the embedding method consistently in knowledge base completion (and, obviously, more so when entailed axioms are considered as positives during evaluation).

While we only report our experiments with *ELEmbeddings*, our findings, in particular about the evaluation and use of deductive closure, are applicable to other geometric ontology embedding methods. As ontology embedding methods are increasingly applied in knowledge-enhanced learning and other tasks that utilize some form of approximate computation of entailments, our results can also serve to improve the applications of ontology embeddings.

## Bibliography

- [1] Baader, F., Brandt, S., Lutz, C.: Pushing the  $\mathcal{EL}$  envelope. In: Proceedings of the Nineteenth International Joint Conference on Artificial Intelligence IJCAI-05. Morgan-Kaufmann Publishers, Edinburgh, UK (2005)
- [2] Baader, F., Calvanese, D., McGuinness, D., Nardi, D., Patel-Schneider, P.F. (eds.): The Description Logic Handbook: Theory, Implementation, and Applications. Cambridge University Press (2003)
- [3] Bouraoui, Z., Jameel, S., Schockaert, S.: Inductive reasoning about ontologies using conceptual spaces. Proceedings of the AAAI Conference on Artificial Intelligence **31**(1) (Feb 2017). <https://doi.org/10.1609/aaai.v31i1.11162>, <http://dx.doi.org/10.1609/aaai.v31i1.11162>
- [4] Cao, P., Hao, Y., Chen, Y., Liu, K., Xu, J., Li, H., Jiang, X., Zhao, J.: Event ontology completion with hierarchical structure evolution networks. In: Bouamor, H., Pino, J., Bali, K. (eds.) Proceedings of the 2023 Conference on Empirical Methods in Natural Language Processing. pp. 306–320. Association for Computational Linguistics, Singapore (Dec 2023). <https://doi.org/10.18653/v1/2023.emnlp-main.21>, <https://aclanthology.org/2023.emnlp-main.21>
- [5] Chen, J., Hu, P., Jimenez-Ruiz, E., Holter, O.M., Antonyrajah, D., Horrocks, I.: OWL2Vec\*: embedding of OWL ontologies. Machine Learning (Jun 2021). <https://doi.org/10.1007/s10994-021-05997-6>
- [6] Chen, J., Althagafi, A., Hoehndorf, R.: Predicting candidate genes from phenotypes, functions and anatomical site of expression. Bioinformatics **37**(6), 853–860 (Oct 2020). <https://doi.org/10.1093/bioinformatics/btaa879>
- [7] Chen, Z., Wang, Y., Zhao, B., Cheng, J., Zhao, X., Duan, Z.: Knowledge graph completion: A review. Ieee Access **8**, 192435–192456 (2020)
- [8] Consortium, G.O.: Gene ontology consortium: going forward. Nucleic acids research **43**(D1), D1049–D1056 (2015)
- [9] Devlin, J., Chang, M., Lee, K., Toutanova, K.: BERT: pre-training of deep bidirectional transformers for language understanding. In: Burstein, J., Doran, C., Solorio, T. (eds.) Proceedings of the 2019 Conference of the North American Chapter of the Association for Computational Linguistics: Human Language Technologies, NAACL-HLT 2019, Minneapolis, MN, USA, June 2-7, 2019, Volume 1 (Long and Short Papers). pp. 4171–4186. Association for Computational Linguistics (2019). <https://doi.org/10.18653/V1/N19-1423>, <https://doi.org/10.18653/v1/n19-1423>
- [10] d’Amato, C., Fanizzi, N., Fazzinga, B., Gottlob, G., Lukasiewicz, T.: Ontology-based semantic search on the web and its combination with the power of inductive reasoning. Annals of Mathematics and Artificial Intelligence **65**(2-3), 83–121 (Jul 2012). <https://doi.org/10.1007/s10472-012-9309-7>, <http://dx.doi.org/10.1007/s10472-012-9309-7>

- [11] Golbreich, C., Horrocks, I.: The OBO to OWL mapping, GO to OWL 1.1! In: Golbreich, C., Kalyanpur, A., Parsia, B. (eds.) Proceedings of the OWLED 2007 Workshop on OWL: Experiences and Directions, Innsbruck, Austria, June 6-7, 2007. CEUR Workshop Proceedings, vol. 258. CEUR-WS.org (2007), <https://ceur-ws.org/Vol-258/paper35.pdf>
- [12] Hinnerichs, T., Hoehndorf, R.: Dti-voodoo: machine learning over interaction networks and ontology-based background knowledge predicts drug-target interactions. *Bioinformatics* **37**(24), 4835–4843 (Jul 2021). <https://doi.org/10.1093/bioinformatics/btab548>, <http://dx.doi.org/10.1093/bioinformatics/btab548>
- [13] Jackermeier, M., Chen, J., Horrocks, I.: Dual box embeddings for the description logic EL++. In: Proceedings of the ACM Web Conference 2024. WWW '24 (2024). <https://doi.org/10.1145/3589334.3645648>
- [14] Ji, Q., Qi, G., Ye, Y., Li, J., Li, S., Ren, J., Lu, S.: Ontology revision based on pre-trained language models (2023)
- [15] Jiang, X., Huang, Y., Nickel, M., Tresp, V.: Combining Information Extraction, Deductive Reasoning and Machine Learning for Relation Prediction, p. 164–178. Springer Berlin Heidelberg (2012). [https://doi.org/10.1007/978-3-642-30284-8\\_18](https://doi.org/10.1007/978-3-642-30284-8_18), [http://dx.doi.org/10.1007/978-3-642-30284-8\\_18](http://dx.doi.org/10.1007/978-3-642-30284-8_18)
- [16] Kazakov, Y., Krötzsch, M., Simančík, F.: The incredible ELK. *Journal of Automated Reasoning* **53**(1), 1–61 (Nov 2013). <https://doi.org/10.1007/s10817-013-9296-3>
- [17] Kingma, D.P., Ba, J.: Adam: A method for stochastic optimization. In: Bengio, Y., LeCun, Y. (eds.) 3rd International Conference on Learning Representations, ICLR 2015, San Diego, CA, USA, May 7-9, 2015, Conference Track Proceedings (2015)
- [18] Kulmanov, M., Liu-Wei, W., Yan, Y., Hoehndorf, R.: El embeddings: Geometric construction of models for the description logic el ++. In: International Joint Conference on Artificial Intelligence (2019)
- [19] Li, N., Bailleux, T., Bouraoui, Z., Schockaert, S.: Ontology completion with natural language inference and concept embeddings: An analysis (2024)
- [20] Mendez, J.: jcel: A modular rule-based reasoner. In: Horrocks, I., Yatskevich, M., Jiménez-Ruiz, E. (eds.) Proceedings of the 1st International Workshop on OWL Reasoner Evaluation (ORE-2012), Manchester, UK, July 1st, 2012. CEUR Workshop Proceedings, vol. 858. CEUR-WS.org (2012), [https://ceur-ws.org/Vol-858/ore2012\\_paper12.pdf](https://ceur-ws.org/Vol-858/ore2012_paper12.pdf)
- [21] Mering, C.v.: String: a database of predicted functional associations between proteins. *Nucleic Acids Research* **31**(1), 258–261 (Jan 2003). <https://doi.org/10.1093/nar/gkg034>, <http://dx.doi.org/10.1093/nar/gkg034>
- [22] Mežnar, S., Bevec, M., Lavrač, N., Škrlić, B.: Ontology completion with graph-based machine learning: A comprehensive evaluation. *Machine Learning and Knowledge Extraction* **4**(4), 1107–1123 (Dec 2022). <https://doi.org/10.3390/make4040056>, <http://dx.doi.org/10.3390/make4040056>

- [23] Mondal, S., Bhatia, S., Mutharaju, R.: Emel++: Embeddings for EL++ description logic. In: Martin, A., Hinkelmann, K., Fill, H., Gerber, A., Lenat, D., Stolle, R., van Harmelen, F. (eds.) Proceedings of the AAAI 2021 Spring Symposium on Combining Machine Learning and Knowledge Engineering (AAAI-MAKE 2021), Stanford University, Palo Alto, California, USA, March 22-24, 2021. CEUR Workshop Proceedings, vol. 2846. CEUR-WS.org (2021)
- [24] Özcepe, O.L., Leemhuis, M., Wolter, D.: Embedding ontologies in the description logic alc by axis-aligned cones. *Journal of Artificial Intelligence Research* **78**, 217–267 (Oct 2023). <https://doi.org/10.1613/jair.1.13939>, <http://dx.doi.org/10.1613/jair.1.13939>
- [25] Peng, X., Tang, Z., Kulmanov, M., Niu, K., Hoehndorf, R.: Description logic el++ embeddings with intersectional closure (2022)
- [26] Radivojac, P., Clark, W.T.: Information-theoretic evaluation of predicted ontological annotations. *Bioinformatics* **29**(13), i53–i61 (06 2013). <https://doi.org/10.1093/bioinformatics/btt228>, <https://doi.org/10.1093/bioinformatics/btt228>
- [27] Sato, Y., Stapleton, G., Jamnik, M., Shams, Z.: Deductive reasoning about expressive statements using external graphical representations. In: Proceedings of the 40th Annual Conference of the Cognitive Science Society. pp. 0–0. Cognitive Science Society (Jul 2018), cogSci 2018 ; Conference date: 25-07-2018 Through 28-07-2018
- [28] Shiraiishi, Y., Kaneiwa, K.: A self-matching training method with annotation embedding models for ontology subsumption prediction (2024)
- [29] Wang, Q., Mao, Z., Wang, B., Guo, L.: Knowledge graph embedding: A survey of approaches and applications. *IEEE transactions on knowledge and data engineering* **29**(12), 2724–2743 (2017)
- [30] Xiong, B., Potyka, N., Tran, T.K., Nayyeri, M., Staab, S.: Faithful embeddings for EL++ knowledge bases. In: Proceedings of the 21st International Semantic Web Conference (ISWC2022). pp. 1–18 (2022)
- [31] Zhapa-Camacho, F., Hoehndorf, R.: From axioms over graphs to vectors, and back again: evaluating the properties of graph-based ontology embeddings (2023)
- [32] Zhapa-Camacho, F., Kulmanov, M., Hoehndorf, R.: mOWL: Python library for machine learning with biomedical ontologies. *Bioinformatics* (12 2022). <https://doi.org/10.1093/bioinformatics/btac811>, <https://doi.org/10.1093/bioinformatics/btac811>, btac811

## Appendix

### A Naive model construction

Similarly to [12] we construct  $n \times n$  PPI and  $n \times m$  function prediction matrices  $M_{iw}$  and  $M_{hf}$  respectively:  $M_{iw}(P_1, P_2) = 1$  if  $\{P_1\} \sqsubseteq \exists \textit{interacts\_with}.\{P_2\}$  is in the train set for PPI and 0 otherwise, and  $M_{hf}(P, GO) = 1$  if  $\{P\} \sqsubseteq \exists \textit{has\_function}.\{GO\}$  is in the train set for function prediction (0 otherwise). Assuming that *interacts\_with* relation is symmetric we additionally design matrix  $M'_{iw}$  for human data where  $M'_{iw}(P_1, P_2) = M'_{iw}(P_2, P_1) = 1$  when  $\{P_1\} \sqsubseteq \exists \textit{interacts\_with}.\{P_2\}$  or  $\{P_2\} \sqsubseteq \exists \textit{interacts\_with}.\{P_1\}$  can be found in the train part of the dataset. Scoring function used for rank-based predictions is described in section 4.4.

### B GCI statistics

Table 3: Datasets' statistics

Dataset name	GCI type	Number of axioms
Yeast	$C \sqsubseteq D$	81,068
	$C \sqsubseteq \perp$	0
	$C \cap D \sqsubseteq E$	11,825
	$C \cap D \sqsubseteq \perp$	31
	$C \sqsubseteq \exists R.D$	293,645
	$\exists R.C \sqsubseteq D$	11,823
	$\exists R.C \sqsubseteq \perp$	0
Human	$C \sqsubseteq D$	87,555
	$C \sqsubseteq \perp$	0
	$C \cap D \sqsubseteq E$	12,154
	$C \cap D \sqsubseteq \perp$	30
	$C \sqsubseteq \exists R.D$	958,674
	$\exists R.C \sqsubseteq D$	12,152
	$\exists R.C \sqsubseteq \perp$	0

**C Hyperparameters**

Table 4: Best models' hyperparameters, Yeast iw dataset

Experiment	Best hyperparameters
<i>ELEmbeddings</i> original	embed_dim = 200 $\gamma = 0.1$ learning_rate = 0.01
LeakyReLU + relaxed regularization	embed_dim = 50 $\gamma = 0.1$ $R = 1$ learning_rate = 0.01
GCI0-GCI3 negative losses	embed_dim = 50 $\gamma = 0.1$ $R = 2$ learning_rate = 0.01
Filtered negatives	embed_dim = 100 $\gamma = 0.1$ $R = 1$ learning_rate = 0.01

Table 5: Best models' hyperparameters, Yeast hf dataset

Experiment	Best hyperparameters
<i>ELEmbeddings</i> original	embed_dim = 400 $\gamma = 0.1$ learning_rate = 0.001
LeakyReLU + relaxed regularization	embed_dim = 100 $\gamma = 0.1$ $R = 2$ learning_rate = 0.0001
GCI0-GCI3 negative losses	embed_dim = 200 $\gamma = 0.1$ $R = 1$ learning_rate = 0.0001
Filtered negatives	embed_dim = 200 $\gamma = 0.1$ $R = 1$ learning_rate = 0.0001

Table 6: Best models' hyperparameters, Human iw dataset

Experiment	Best hyperparameters
<i>ELEmbeddings</i> original	embed_dim = 400 $\gamma = 0.1$ learning_rate = 0.001
LeakyReLU + relaxed regularization	embed_dim = 100 $\gamma = 0.01$ $R = 1$ learning_rate = 0.0001
GCI0-GCI3 negative losses	embed_dim = 200 $\gamma = 0.1$ $R = 2$ learning_rate = 0.001
Filtered negatives	embed_dim = 200 $\gamma = 0.1$ $R = 2$ learning_rate = 0.001

Table 7: Best models' hyperparameters, Human hf dataset

Experiment	Best hyperparameters
<i>ELEmbeddings</i> original	embed_dim = 50 $\gamma = 0.1$ learning_rate = 0.001
LeakyReLU + relaxed regularization	embed_dim = 50 $\gamma = 0.1$ $R = 2$ learning_rate = 0.0001
GCI0-GCI3 negative losses	embed_dim = 400 $\gamma = 0.1$ $R = 2$ learning_rate = 0.0001
Filtered negatives	embed_dim = 400 $\gamma = 0.1$ $R = 2$ learning_rate = 0.0001

## D Ablation study hyperparameters

Table 8: Best models' hyperparameters for ablation study, Yeast iw dataset

Experiment	Best hyperparameters
LeakyReLU	embed_dim = 200 $\gamma = 0.1$ learning_rate = 0.01
GCI0-GCI3 negative losses	embed_dim = 100 $\gamma = 0.1$ learning_rate = 0.01
Relaxed regularization	embed_dim = 100 $\gamma = 0.01$ $R = 1$ learning_rate = 0.01
Filtered negatives	embed_dim = 400 $\gamma = 0.01$ learning_rate = 0.01

Table 9: Best models' hyperparameters for ablation study, Yeast hf dataset

Experiment	Best hyperparameters
LeakyReLU	embed_dim = 400 $\gamma = -0.1$ learning_rate = 0.0001
GCI0-GCI3 negative losses	embed_dim = 200 $\gamma = 0.1$ learning_rate = 0.01
Relaxed regularization	embed_dim = 200 $\gamma = 0.1$ $R = 1$ learning_rate = 0.01
Filtered negatives	embed_dim = 400 $\gamma = 0.1$ learning_rate = 0.001

Table 10: Best models' hyperparameters for ablation study, Human iw dataset

Experiment	Best hyperparameters
LeakyReLU	embed_dim = 50 $\gamma = -0.1$ learning_rate = 0.0001
GCI0-GCI3 negative losses	embed_dim = 200 $\gamma = 0.1$ learning_rate = 0.001
Relaxed regularization	embed_dim = 400 $\gamma = 0.1$ $R = 1$ learning_rate = 0.001
Filtered negatives	embed_dim = 400 $\gamma = 0.1$ learning_rate = 0.001

Table 11: Best models' hyperparameters for ablation study, Human hf dataset

Experiment	Best hyperparameters
LeakyReLU	embed_dim = 50 $\gamma = 0.01$ learning_rate = 0.01
GCI0-GCI3 negative losses	embed_dim = 400 $\gamma = 0.1$ learning_rate = 0.001
Relaxed regularization	embed_dim = 400 $\gamma = 0.01$ $R = 2$ learning_rate = 0.01
Filtered negatives	embed_dim = 50 $\gamma = 0.1$ learning_rate = 0.001

## E Detailed results of different settings of *ELEmbeddings*

*ELEmbeddings* experiments: the first column corresponds to the original model, the second one – to LeakyReLU replacement and soft regularization, the third – to GCI0-GCI3 losses added, and, finally, the last one – to negatives filtering. *iw* refers to *interacts\_with* dataset, *hf* – to *has\_function* dataset.

		ReLU	Leaky+Reg	Losses	Neg. filter
Yeast iw	Hits@10	0.00	<b>0.09</b>	<b>0.09</b>	<b>0.09</b>
	FHits@10	0.00	0.26	0.25	<b>0.29</b>
	Hits@100	0.15	0.52	0.52	<b>0.55</b>
	FHits@100	0.15	0.74	0.74	<b>0.78</b>
	macro_MR	287.36	242.76	245.21	<b>231.70</b>
	micro_MR	359.70	310.93	310.46	<b>296.12</b>
	macro_FMR	287.06	182.93	185.81	<b>172.80</b>
	micro_FMR	359.61	280.76	280.44	<b>266.51</b>
	macro_AUC	0.95	<b>0.96</b>	<b>0.96</b>	<b>0.96</b>
	micro_AUC	0.95	<b>0.96</b>	<b>0.96</b>	<b>0.96</b>
	macro_FAUC	0.95	<b>0.97</b>	<b>0.97</b>	<b>0.97</b>
	micro_FAUC	0.95	<b>0.97</b>	0.96	0.96

		ReLU	Leaky+Reg	Losses	Neg. filter
Yeast hf	Hits@10	0.00	<b>0.22</b>	0.21	0.21
	FHits@10	0.00	<b>0.25</b>	0.23	0.24
	Hits@100	0.00	<b>0.54</b>	<b>0.54</b>	0.53
	FHits@100	0.00	<b>0.55</b>	0.54	0.54
	macro_MR	5183.02	3215.76	<b>2873.35</b>	2879.59
	micro_MR	5205.98	3174.81	<b>2850.97</b>	2858.37
	macro_FMR	5183.01	3211.80	<b>2869.43</b>	2875.67
	micro_FMR	5205.97	3171.08	<b>2847.28</b>	2854.69
	macro_AUC	0.90	<b>0.94</b>	<b>0.94</b>	<b>0.94</b>
	micro_AUC	0.90	0.94	<b>0.95</b>	<b>0.95</b>
	macro_FAUC	0.90	<b>0.94</b>	<b>0.94</b>	<b>0.94</b>
	micro_FAUC	0.90	0.94	<b>0.95</b>	<b>0.95</b>

		ReLU	Leaky+Reg	Losses	Neg. filter
Human iw	Hits@10	0.00	<b>0.01</b>	0.00	0.00
	FHits@10	0.00	<b>0.02</b>	0.00	0.00
	Hits@100	0.03	0.12	0.26	<b>0.32</b>
	FHits@100	0.03	0.24	0.50	<b>0.63</b>
	macro_MR	490.14	1440.09	338.67	<b>277.22</b>
	micro_MR	513.98	1973.29	339.97	<b>283.61</b>
	macro_FMR	490.09	1361.12	258.17	<b>196.76</b>
	micro_FMR	513.97	1936.41	302.18	<b>245.83</b>
	macro_AUC	0.97	0.93	0.98	0.99
	micro_AUC	0.97	0.91	0.98	0.99
	macro_FAUC	0.97	0.93	<b>0.99</b>	<b>0.99</b>
	micro_FAUC	0.97	0.91	<b>0.99</b>	<b>0.99</b>

		ReLU	Leaky+Reg	Losses	Neg. filter
Human hf	Hits@10	0.00	<b>0.13</b>	0.06	0.06
	FHits@10	0.00	<b>0.14</b>	0.06	0.06
	Hits@100	0.00	<b>0.34</b>	0.28	0.28
	FHits@100	0.00	<b>0.35</b>	0.28	0.28
	macro_MR	7642.19	4070.90	2281.62	<b>2272.33</b>
	micro_MR	7645.75	3578.47	1972.00	<b>1963.87</b>
	macro_FMR	7642.15	4059.81	2270.35	<b>2261.06</b>
	micro_FMR	7645.73	3570.33	1963.76	<b>1955.62</b>
	macro_AUC	0.85	0.92	<b>0.95</b>	<b>0.95</b>
	micro_AUC	0.85	0.94	<b>0.97</b>	<b>0.97</b>
	macro_FAUC	0.85	0.92	<b>0.95</b>	<b>0.95</b>
	micro_FAUC	0.85	0.94	<b>0.97</b>	<b>0.97</b>

## F Detailed results of comparison with the “naive” classifier.

Naive approach vs *ELEmbeddings* with LeakyReLU, soft regularization constraints, GCI0-GCI3 negative losses and filtered negatives. *iw* refers to *interacts\_with* dataset, *hf* to *has\_function* dataset. For Human iw dataset we report here metrics both for  $M'_{iw}$  and  $M_{iw}$ , *sym* here corresponds to the symmetric Human iw dataset (for further details see Appendix (section A)).

Note that by definition filtered metrics should be less than or equal to corresponding non-filtered metrics, yet here filtered naive AUC ROC is less than non-filtered one. The reason is trapezoidal rule for numerical integration used to calculate AUC ROC based on FPR and TPR points: due to the facts that the number of different rank values is relatively small compared to the number of GO classes and that the score relies exclusively on the number of proteins having the function, it provides the grid not accurate enough, and the same non-filtered rank converts into multiple lower ranks while filtered forming more well-suited computational grid.

		Naive	ELEm
Yeast iw	Hits@10	0.01	<b>0.09</b>
	FHits@10	0.05	<b>0.29</b>
	Hits@100	0.12	<b>0.55</b>
	FHits@100	0.23	<b>0.78</b>
	macro_MR	1228.68	<b>231.70</b>
	micro_MR	1845.96	<b>296.12</b>
	macro_FMR	1174.33	<b>172.80</b>
	micro_FMR	1819.47	<b>266.51</b>
	macro_AUC	0.80	<b>0.96</b>
	micro_AUC	0.72	<b>0.96</b>
	macro_FAUC	0.81	<b>0.97</b>
	micro_FAUC	0.72	<b>0.96</b>

		Naive	ELEm
Yeast hf	Hits@10	0.20	<b>0.21</b>
	FHits@10	0.21	<b>0.24</b>
	Hits@100	0.40	<b>0.53</b>
	FHits@100	0.41	<b>0.54</b>
	macro_MR	<b>2694.33</b>	2879.59
	micro_MR	<b>2658.51</b>	2858.37
	macro_FMR	<b>2690.58</b>	2875.67
	micro_FMR	<b>2654.98</b>	2854.69
	macro_AUC	<b>0.97</b>	0.94
	micro_AUC	0.95	0.95
	macro_FAUC	<b>0.95</b>	0.94
	micro_FAUC	0.95	0.95

		Naive	ELEm
Human iw (sym)	Hits@10	<b>0.01</b>	0.00
	FHits@10	<b>0.02</b>	0.00
	Hits@100	0.07	<b>0.32</b>
	FHits@100	0.08	<b>0.63</b>
	macro_MR	2377.39	<b>277.22</b>
	micro_MR	3313.50	<b>283.61</b>
	macro_FMR	2299.09	<b>196.76</b>
	micro_FMR	3276.97	<b>245.83</b>
	macro_AUC	0.88	<b>0.99</b>
	micro_AUC	0.84	<b>0.99</b>
	macro_FAUC	0.88	<b>0.99</b>
	micro_FAUC	0.85	<b>0.99</b>

		Naive	ELEm
Human iw (non-sym)	Hits@10	<b>0.01</b>	0.00
	FHits@10	<b>0.02</b>	0.00
	Hits@100	0.07	<b>0.32</b>
	FHits@100	0.08	<b>0.63</b>
	macro_MR	2433.80	<b>277.22</b>
	micro_MR	3412.09	<b>283.61</b>
	macro_FMR	2353.87	<b>196.76</b>
	micro_FMR	3374.88	<b>245.83</b>
	macro_AUC	0.88	<b>0.99</b>
	micro_AUC	0.84	<b>0.99</b>
	macro_FAUC	0.88	<b>0.99</b>
	micro_FAUC	0.84	<b>0.99</b>

		Naive	ELEm
Human hf	Hits@10	<b>0.16</b>	0.06
	FHits@10	<b>0.18</b>	0.06
	Hits@100	<b>0.39</b>	0.28
	FHits@100	<b>0.39</b>	0.28
	macro_MR	<b>1978.53</b>	2272.33
	micro_MR	<b>1785.81</b>	1963.87
	macro_FMR	<b>1967.45</b>	2261.06
	micro_FMR	<b>1777.73</b>	1955.62
	macro_AUC	<b>0.97</b>	<b>0.95</b>
	micro_AUC	0.97	<b>0.97</b>
	macro_FAUC	<b>0.96</b>	0.95
	micro_FAUC	0.97	<b>0.97</b>

## G Ablation study

*ELEmbeddings* experiments: the first column corresponds to the original model, the second one – to LeakyReLU replacement, the third one – to soft regularization, the fourth – to GCI0-GCI3 losses, and, finally, the last one – to negatives filtering. *iw* refers to *interacts\_with* dataset, *hf* – to *has\_function* dataset. Best hyperparameters for these experiments can be found in Appendix D.

		ReLU	LeakyReLU	Reg	Losses	Neg. filter
Yeast iw	Hits@10	0.00	0.09	0.00	0.00	0.00
	FHits@10	0.00	0.27	0.00	0.00	0.00
	Hits@100	0.15	0.54	0.11	0.14	0.11
	FHits@100	0.15	0.76	0.11	0.14	0.11
	macro_MR	287.36	236.67	309.77	329.22	327.87
	micro_MR	359.70	301.79	378.44	409.94	415.26
	macro_FMR	287.06	176.64	309.59	328.86	327.87
	micro_FMR	359.61	271.57	378.38	409.83	415.26
	macro_AUC	0.95	0.96	0.95	0.95	0.95
	micro_AUC	0.95	0.96	0.94	0.94	0.94
	macro_FAUC	0.95	0.97	0.95	0.95	0.95
	micro_FAUC	0.95	0.96	0.94	0.94	0.94

		ReLU	LeakyReLU	Reg	Losses	Neg. filter
Yeast hf	Hits@10	0.00	0.25	0.00	0.00	0.00
	FHits@10	0.00	0.28	0.00	0.00	0.00
	Hits@100	0.00	0.54	0.00	0.00	0.00
	FHits@100	0.00	0.55	0.00	0.00	0.00
	macro_MR	5183.02	2770.44	8252.35	3450.22	5287.68
	micro_MR	5205.98	2752.54	8221.89	3426.88	5311.96
	macro_FMR	5183.01	2766.28	8252.33	3450.21	5287.67
	micro_FMR	5205.97	2748.63	8221.88	3426.87	5311.95
	macro_AUC	0.90	0.95	0.84	0.93	0.90
	micro_AUC	0.90	0.95	0.84	0.93	0.90
	macro_FAUC	0.90	0.95	0.84	0.93	0.90
	micro_FAUC	0.90	0.95	0.84	0.93	0.90

		ReLU	LeakyReLU	Reg	Losses	Neg. filter
Human iw	Hits@10	0.00	0.03	0.00	0.00	0.00
	FHits@10	0.00	0.09	0.00	0.00	0.00
	Hits@100	0.03	0.24	0.00	0.04	0.03
	FHits@100	0.03	0.40	0.00	0.04	0.03
	macro_MR	490.14	1723.06	565.83	551.94	508.93
	micro_MR	513.98	2904.69	602.37	545.95	514.27
	macro_FMR	490.09	1642.98	565.80	551.89	508.92
	micro_FMR	513.97	2866.92	602.36	545.93	514.27
	macro_AUC	0.97	0.91	0.97	0.97	0.97
	micro_AUC	0.97	0.87	0.97	0.97	0.97
	macro_FAUC	0.97	0.92	0.97	0.97	0.97
	micro_FAUC	0.97	0.87	0.97	0.97	0.97

		ReLU	LeakyReLU	Reg	Losses	Neg. filter
Human hf	Hits@10	0.00	0.05	0.00	0.00	0.00
	FHits@10	0.00	0.06	0.00	0.00	0.00
	Hits@100	0.00	0.25	0.00	0.00	0.00
	FHits@100	0.00	0.26	0.00	0.00	0.00
	macro_MR	7642.19	5143.27	10295.57	3934.28	7617.16
	micro_MR	7645.75	4736.35	10226.14	3881.40	7608.48
	macro_FMR	7642.15	5132.24	10295.54	3934.24	7617.14
	micro_FMR	7645.73	4728.29	10226.12	3881.38	7608.47
	macro_AUC	0.85	0.90	0.79	0.92	0.85
	micro_AUC	0.85	0.92	0.80	0.93	0.85
	macro_FAUC	0.85	0.90	0.79	0.92	0.85
	micro_FAUC	0.85	0.92	0.80	0.93	0.85

## H ROC curves across different models

First, we note that new functionality incorporated into original *ELEmbeddings* model increases the number of axioms localized within top-ranked subset while worsening the ranking of axioms acquiring higher rank which enables more precise model construction, especially for function prediction task. Although ROC curve for PPI prediction in naive case illustrates that the approach falls short compared to other models, it still outperforms *ELEmbeddings* in terms of low-ranked axioms. Additional negative losses carry out on algorithmic efficacy starting from higher-ranked axioms, specially for yeast data. ROC curve for function prediction tasks display the superior performance of naive predictor compared to best learned geometric-based models.

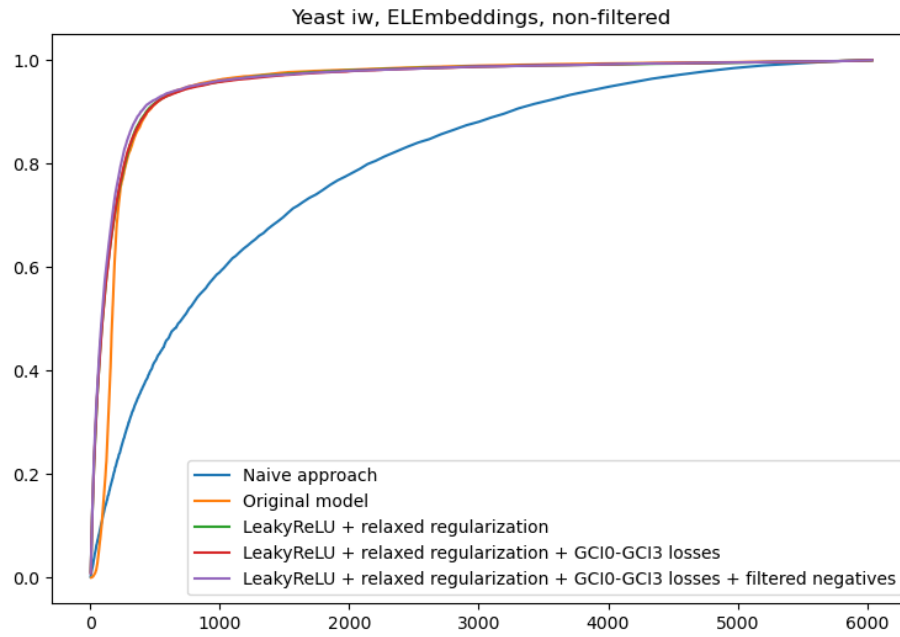


Fig. 1: ROC curves, Yeast iw dataset

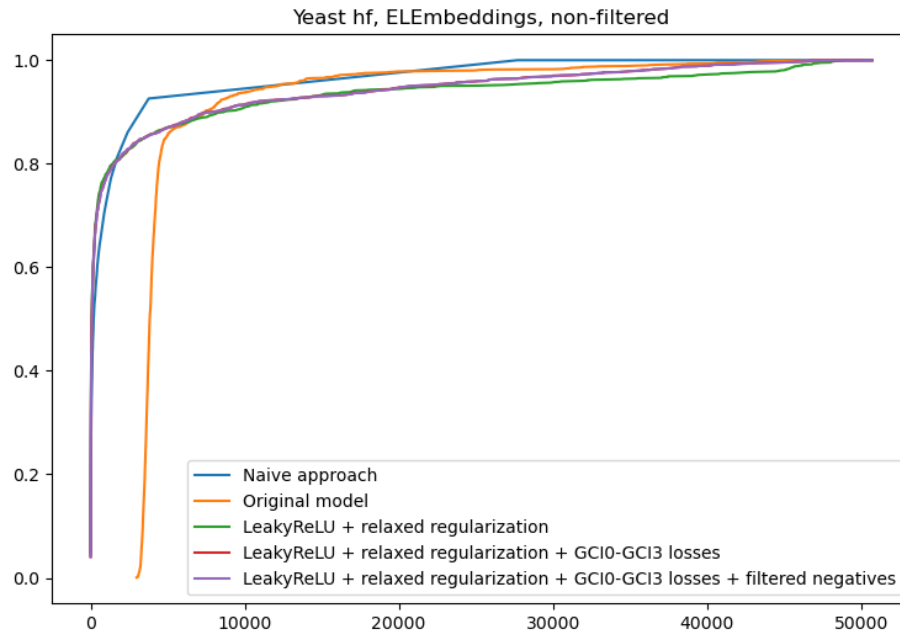


Fig. 2: ROC curves, Yeast hf dataset

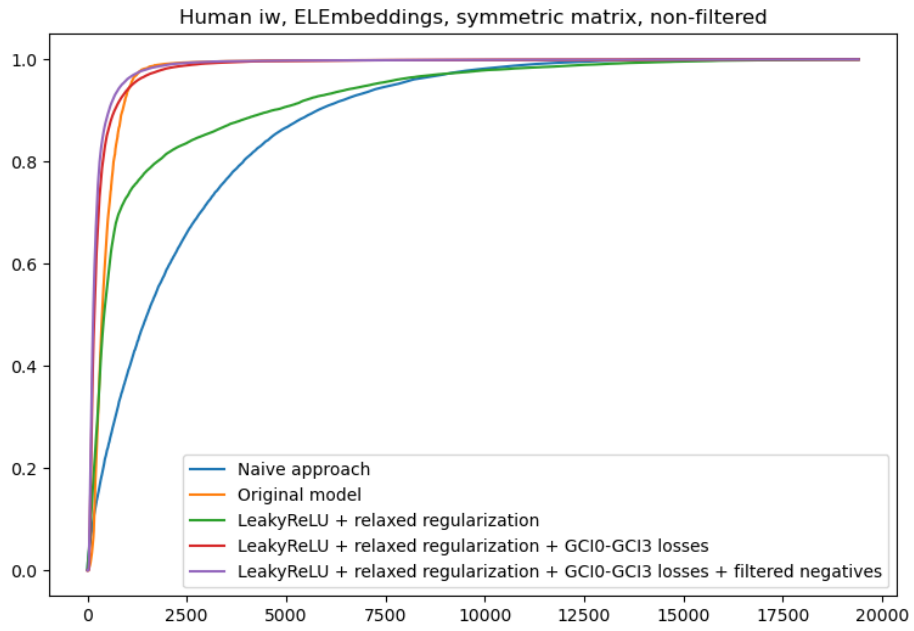


Fig. 3: ROC curves, Human iw dataset

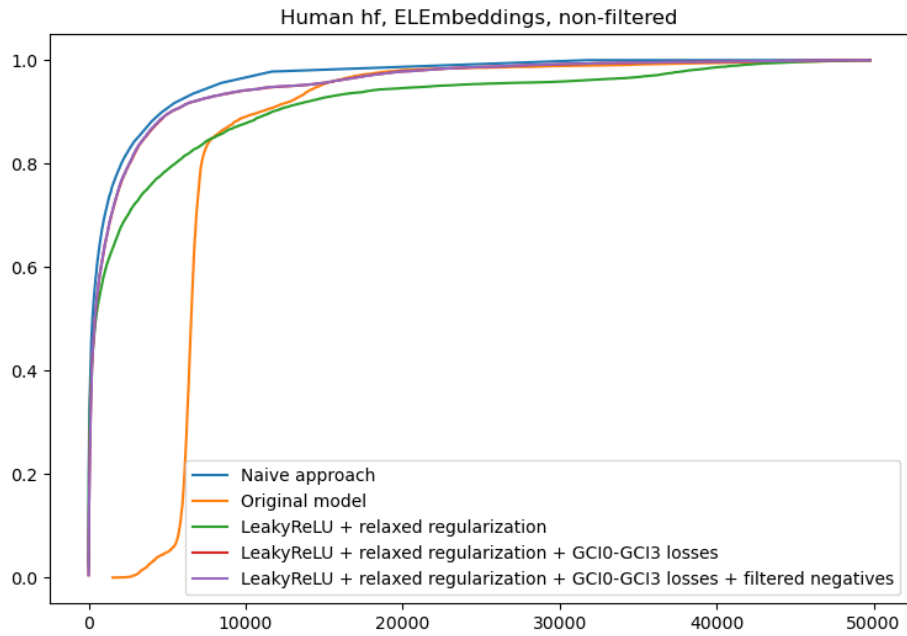


Fig. 4: ROC curves, Human hf dataset

## I ROC curves for LeakyReLU function

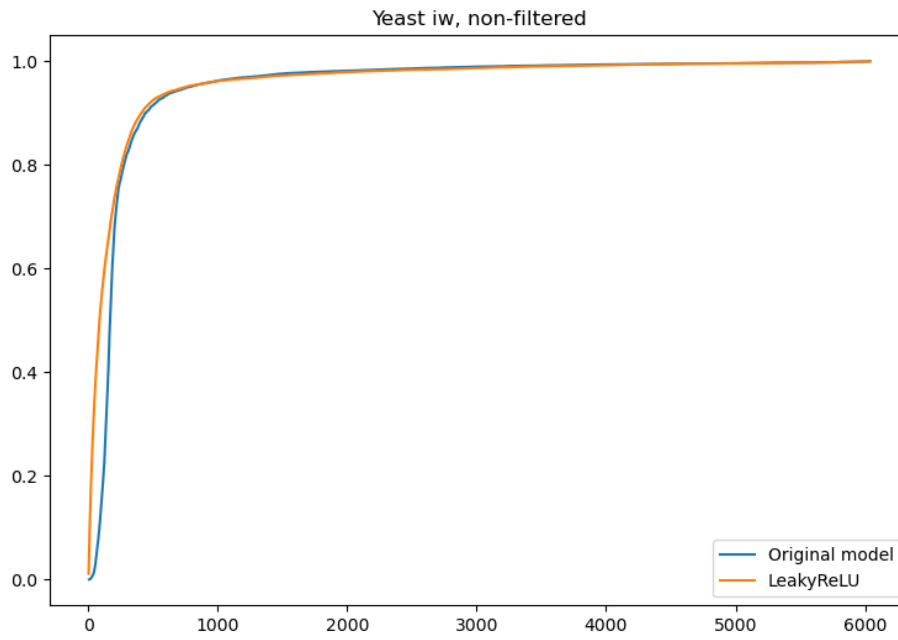


Fig. 5: ROC curves, Yeast iw dataset

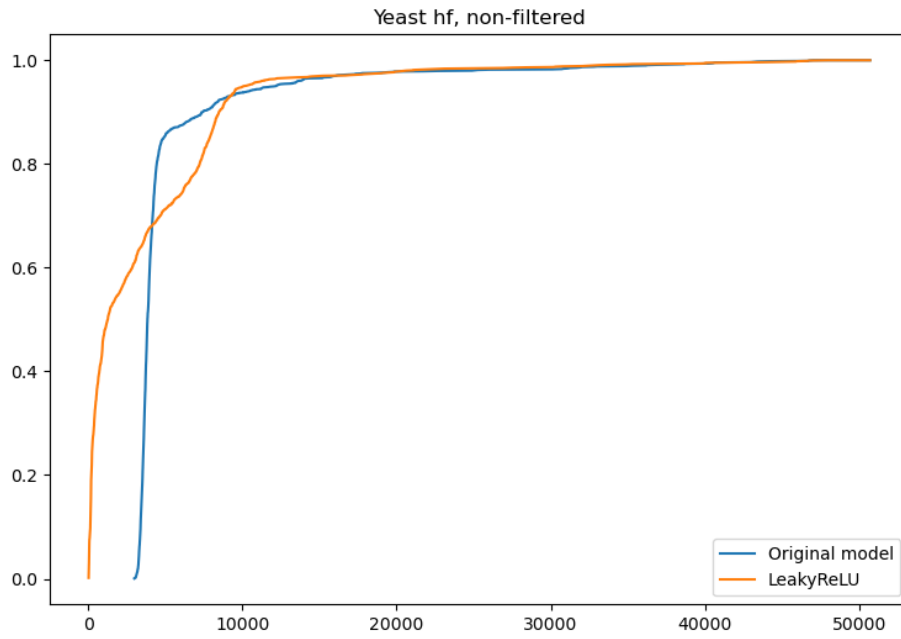


Fig. 6: ROC curves, Yeast hf dataset

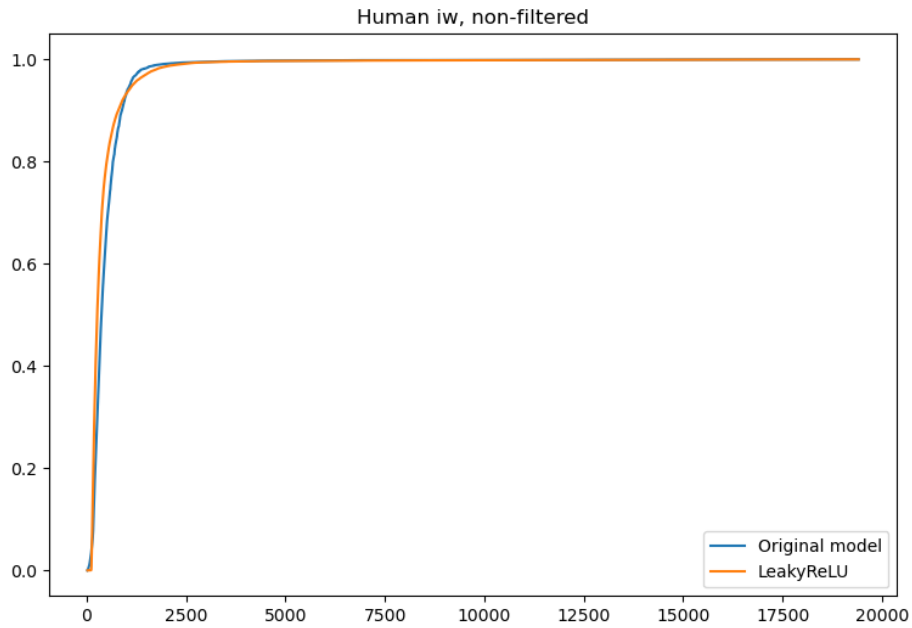


Fig. 7: ROC curves, Human iw dataset

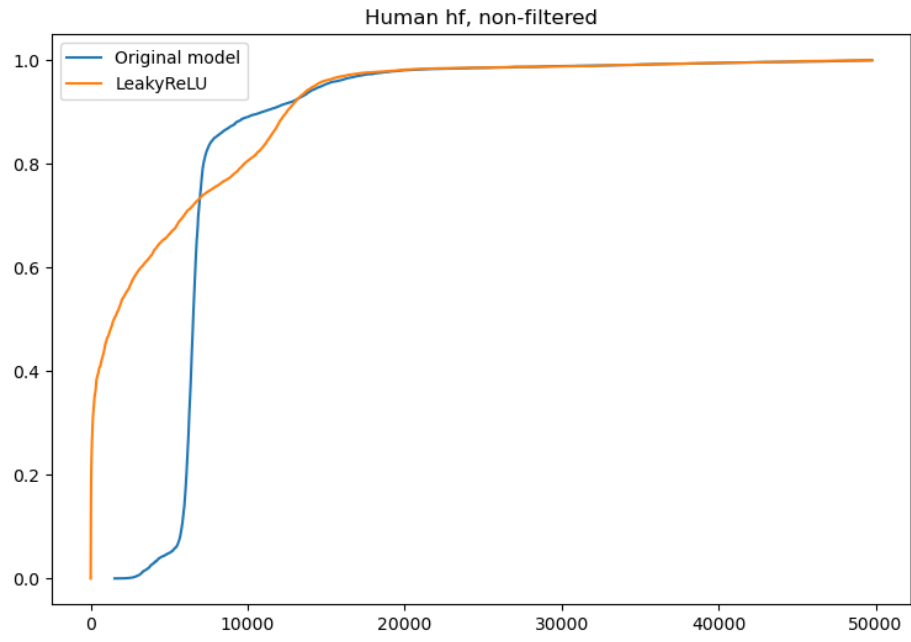


Fig. 8: ROC curves, Human hf dataset

## J Approximate deductive closure

---

**Algorithm 1**

An algorithm for approximate computation of the deductive closure using inference rules; axioms in bold correspond to subclass/superclass axioms derived using ELK reasoner (here we use the transitive closure of the ELK inferences); plain axioms come from the knowledge base.

---

**for** all  $C \sqsubseteq D$  in the knowledge base **do**

$$\frac{C \sqsubseteq D \quad \mathbf{D \sqsubseteq D'}}{C \sqsubseteq D'} \quad \frac{C \sqsubseteq D \quad \mathbf{C' \sqsubseteq C}}{C' \sqsubseteq D}$$

**end for**

**for** all  $C \sqcap D \sqsubseteq E$  in the knowledge base **do**

$$\frac{C \sqcap D \sqsubseteq E \quad \mathbf{C' \sqsubseteq C}}{C' \sqcap D \sqsubseteq E}$$

**end for**

**for** all  $C \sqsubseteq \exists R.D$  in the knowledge base **do**

$$\frac{C \sqsubseteq \exists R.D \quad \mathbf{D \sqsubseteq D'}}{C \sqsubseteq \exists R.D'} \quad \frac{C \sqsubseteq \exists R.D \quad \mathbf{C' \sqsubseteq C}}{C' \sqsubseteq \exists R.D}$$

**end for**

**for** all  $\exists R.C \sqsubseteq D$  in the knowledge base **do**

$$\frac{\exists R.C \sqsubseteq D \quad \mathbf{D \sqsubseteq D'}}{\exists R.C \sqsubseteq D'} \quad \frac{\exists R.C \sqsubseteq D \quad \mathbf{C' \sqsubseteq C}}{\exists R.C' \sqsubseteq D}$$

**end for**

**for** all  $C \sqsubseteq \perp$  in the knowledge base **do**

$$\frac{C \sqsubseteq \perp \quad \mathbf{C' \sqsubseteq C}}{C' \sqsubseteq \perp}$$

**end for**

**for** all  $\exists R.C \sqsubseteq \perp$  in the knowledge base **do**

$$\frac{\exists R.C \sqsubseteq \perp \quad \mathbf{C' \sqsubseteq C}}{\exists R.C' \sqsubseteq \perp}$$

**end for**

---

## K Additional Figures

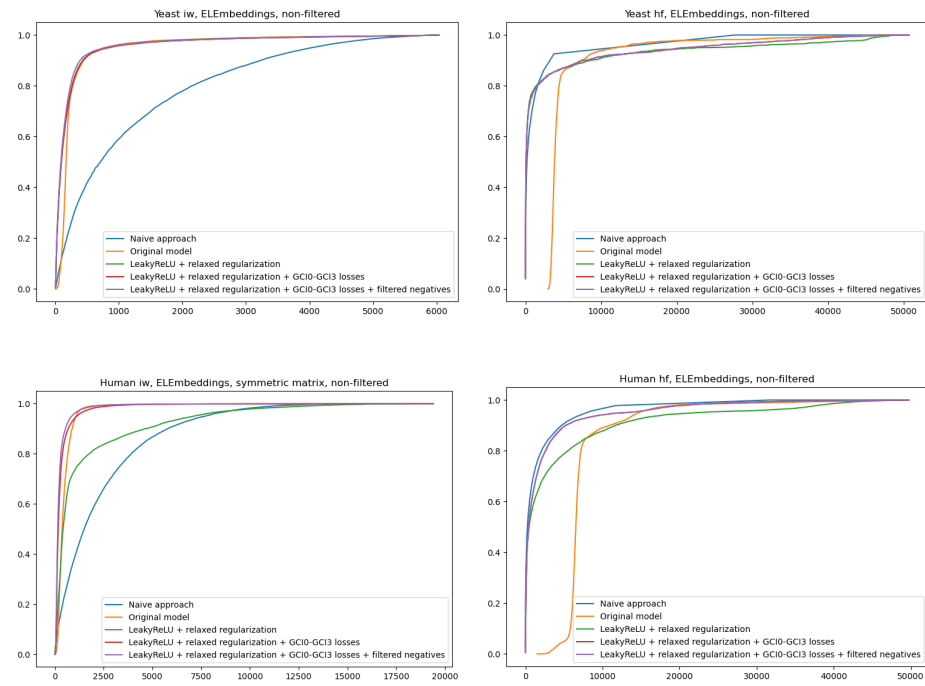


Fig. 9: ROC curves across different models

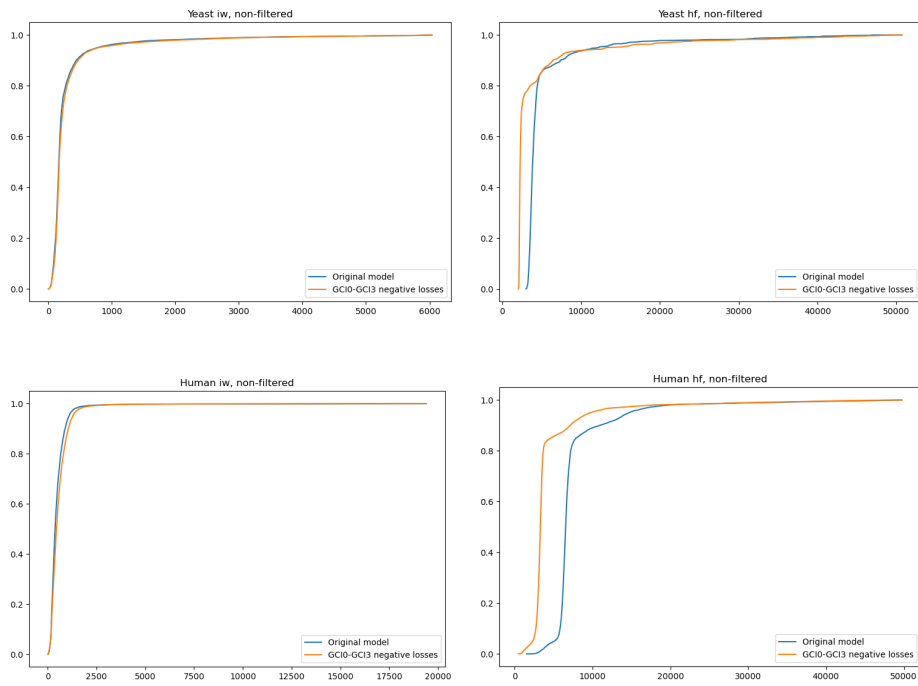


Fig. 10: *ELEmbeddings*, GCI0-GCI3 negative losses vs GCI2 negative loss

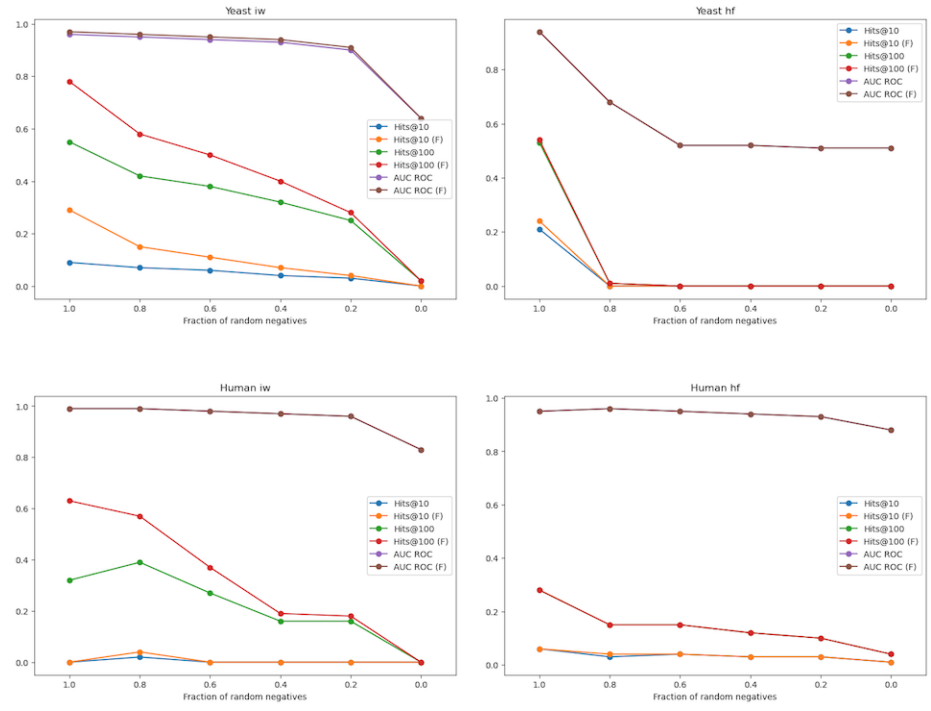


Fig. 11: Random negatives sampling

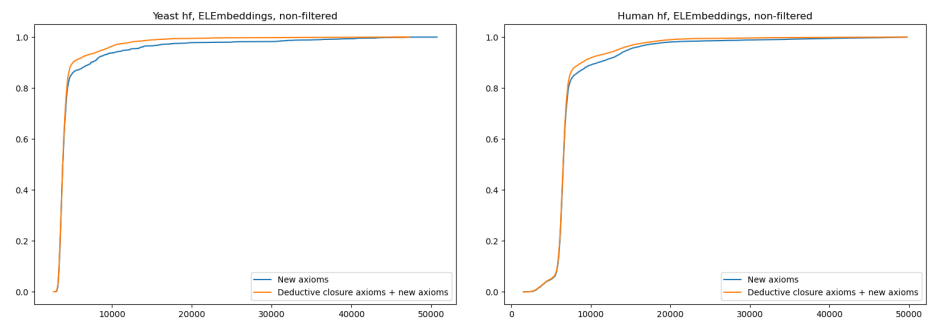


Fig. 12: *ELEMbeddings*, ReLU, ROC curves for entailed axioms and novel axioms

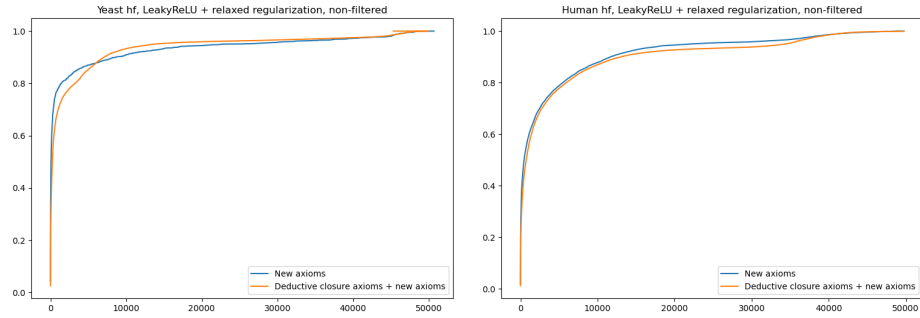


Fig. 13: *EL*Embeddings, LeakyReLU, ROC curves for entailed axioms and novel axioms

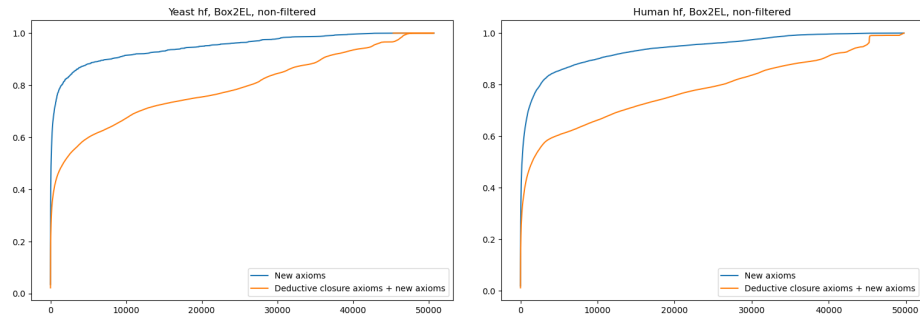


Fig. 14: *Box<sup>2</sup>EL*, ROC curves for entailed axioms and novel axioms